XII International Conference on Textile Composites and Inflatable Structures
STRUCTURAL MEMBRANES 2025
R. Wüchner, A. K. Goldbach, R. Rossi and C. Lázaro (Eds)

ADJOINT-BASED CONSTITUTIVE PARAMETERS IDENTIFICATION IN MEMBRANE STRUCTURES USING DEFORMATION MEASUREMENTS

TALHAH S.A. ANSARI[†,*], SUNETH WARNAKULASURIYA[†], IHAR ANTONAU[§,‖], ANN-KATHRIN GOLDBACH[†], RAINALD LÖHNER[‡,*], HARBIR ANTIL[‡], FACUNDO AIRAUDO[‡] AND ROLAND WÜCHNER[†]

[†] Chair of Structural Analysis, Technical University of Munich, Germany
e-mail: talhah.ansari@tum.de, suneth.warnakulasuriya@tum.de, ann-kathrin.goldbach@tum.de, wuechner@tum.de,

[*] Institute for Advanced Study, Technical University of Munich, D-85748 Garching, Germany

[§] Institute of Structural Analysis, Technical University of Braunschweig, D-38106, Germany
e-mail: ihar.antonau@tu-braunschweig.de

[‖] Cluster of Excellence SE^{2}A – Sustainable and Energy-Efficient Aviation, Technische Universität Braunschweig

[‡] College of Science, George Mason University, Fairfax, Virginia 22030, United States
e-mail: rlohner@gmu.edu, hantil@gmu.edu, fairaudo@gmu.edu

Key words: Pretensioned Membrane Structures, System Identification, Structural Health Monitoring, Pre-Stress Identification, Orthotropic Constitutive Parameters Identification

Summary.

Membrane structures, valued for their flexibility and lightweight nature, are increasingly used in engineering applications. However, their mechanical behavior is challenging to predict due to uncertainties in material properties arising from fabrication methods, environmental exposure, and aging. To address this, we employ an adjoint-based system identification framework that estimates key constitutive parameters and prestress components directly from measurement data. The approach formulates a gradient-based optimization problem, leveraging adjoint sensitivities to efficiently recover material behavior from limited displacement or strain sensor input. In this work, the membrane is modeled using a linear elastic orthotropic material law, thereby introducing four independent constitutive parameters: Young's moduli in the warp and weft directions, Poisson's ratio, and shear modulus. The initial prestress in both directions is also identified, as it significantly influences membrane stability and deformation but often deviates from design values due to fabrication effects. The effectiveness of the approach is demonstrated through two numerical examples: a four-point Hypar and a Conic structure. Numerical investigations show that the proposed method can accurately identify both the constitutive parameters and the prestress state of the membrane. Across all test cases, the relative error in identified parameters remained below 3%, confirming the robustness and precision of the framework even with discrete sensor measurements.

NOMENCLATURE

$J, \mathcal{L}$	=	Cost function and its Lagrangian
$\boldsymbol{\kappa}$	=	System identification parameters
E	=	Young's modulus
$E_{\text{warp}}, E_{\text{weft}}$	=	Young's moduli in warp and weft directions
ν	=	Poisson's ratio
G	=	Shear modulus
$P_{\text{warp}}, P_{\text{weft}}$	=	Membrane Prestress in warp and weft directions
$\boldsymbol{\phi}, \boldsymbol{\phi}^{\text{meas}}$	=	Computed, measured data at the point
$\mathbf{u}^{\text{meas}}$	=	Measured displacement at the point
w	=	Sensor weight
$\mathbf{u}, \tilde{\mathbf{u}}$	=	State and adjoint variables
$\underline{\mathbf{I}}$	=	Displacement, strain interpolation matrices
$\mathbf{R}$	=	FE residual
$\underline{\mathbf{K}}_{\text{tangent}}$	=	Tangent stiffness matrix
$\boldsymbol{\sigma}_0$	=	Initial stress tensor
$\mathbf{f}_{\text{ext}}, \mathbf{f}_{\text{int}}$	=	External and internal force vectors
x	=	scalar value x
$\mathbf{x}$	=	vector x
$\underline{\mathbf{X}}$	=	matrix X

1 INTRODUCTION

Membrane structures are increasingly used in engineering applications such as roofing, tents, and canopies due to their lightweight and flexible nature. However, accurately modeling their mechanical behavior remains challenging because real-world structural membranes exhibit complex characteristics introduced during manufacturing and construction. Variations in weaving patterns, coating techniques, and lamination methods, along with cutting, stitching, and erection procedures, affect the orientation of material axes, introduce local stiffness changes, and redistribute prestress—leading to structural responses that may diverge from those predicted by idealized design models. The conventional membrane design and analysis workflow—formfinding, structural analysis, and cutting pattern generation—typically assumes simplified material behavior and stress states[1]. These assumptions may not reflect the actual conditions present in built structures, underscoring the need for identification methods that can account for construction-induced deviations and support long-term structural health monitoring. Ref. [2] proposed a genetic algorithm-based minimization approach to identify the mechanical properties (orthotropic Young's moduli, Poisson's ratio, and the shear modulus) of rectangular orthotropic membranes through load-displacement data from static membrane bulge tests. Ref. [3] proposed a membrane pretension detection approach based on nonlinear vibration response due to low-velocity pellet impact on the membrane. They derived a formula to calculate the prestension based on the maximum displacement due to the impact. This current work presents an adjoint-based system identification

framework to estimate both constitutive parameters and initial pre-stress states directly from measurement data, enabling model validation and structural health monitoring (SHM). The approach is formulated as a gradient-based optimization problem using adjoint sensitivities for efficient gradient computation. The membrane is modeled with a linear elastic orthotropic law, and the identification targets four constitutive parameters—Young's moduli in warp and weft directions, Poisson's ratio, and shear modulus—alongside directional pre-stress components. This preliminary study focuses on low-fidelity identification, estimating single parameter values for the entire structure. It lays the foundation for future high-resolution investigations involving spatially varying prestress fields and long-term monitoring, where environmental effects such as UV exposure and fatigue may further influence material behavior. Adjoint-based system identification methods have shown success in SHM applications such as damage detection[4], boundary and load identification[5], and thermal field reconstruction[6]. This paper is structured as follows: Sec. 2 presents the adjoint-based framework and the optimization workflow. Sec. 3 illustrates the applicability of the methodology using two numerical examples—a Hypar and a Conic structure—under different prestress, material behavior, and loading conditions. Sec. 4 summarizes the results and outlines remaining challenges.

2 METHODOLOGY

This section describes the proposed methodology for the identification of constitutive and prestress parameters in membrane structures. Section 2.1 presents the adjoint-based method used to frame the system identification problem, and Section 2.2 explains the optimization process.

2.1 Adjoint-based Framework

Let $\boldsymbol{\kappa}$ be the vector of parameters that are to be identified. In this work, $\boldsymbol{\kappa}$ includes the constitutive and prestress parameters governing the mechanical response of the membrane structure. For instance, the constitutive parameters can include Young's modulus, Poisson's ratio, shear modulus, etc. Depending on whether the membrane is modeled using isotropic or orthotropic models, the stiffness can change based on the warp and weft directions. Similarly, the prestresses can also be equal or asymmetric along the warp and weft directions. As an initial step, this work considers linear elastic isotropic and orthotropic materials with both equal and asymmetric prestress states. The developed methodology, however, is general, and intended to be extended to advanced constitutive descriptions, including nonlinearity, hyperelasticity, and anisotropic behaviors.

For a discretized system, this parameter identification problem can be formulated as an optimization challenge with the following generic minimization cost function:

$$J(\mathbf{u}(\boldsymbol{\kappa})) = \frac{1}{2} \sum_{k=1}^{l} \sum_{i=1}^{n} \sum_{j=1}^{m} w_{kij} (\boldsymbol{\phi}_{kij}^{\text{meas}} - \underline{\mathbf{I}}_{kij} \cdot \boldsymbol{\phi}_{ki})^2 \quad , \tag{1}$$

where,

- $k = 1, 2, \ldots, l$ refers to the type of sensor, such as displacement, strain sensors;
- $i = 1, 2, \ldots, n$ refers to the n given load cases;
- $j = 1, 2, \ldots, m$ refers to the m measuring locations of the quantity $\boldsymbol{\phi}_{kij}^{\text{meas}}$;

- $\underline{\mathbf{I}}_{kij}$ refers to the interpolation matrix used to obtain the model response ($\boldsymbol{\phi}_{ki}$) at the measurement points;
- w_{kij} are the individual sensor weights.

In this work, to reduce complexity and to demonstrate the applicability of the approach, only one type of sensor is considered (here, displacement sensors), hence, $l = 1$ and $\boldsymbol{\phi} = \mathbf{u}$. Furthermore, only one load case per system identification is considered to be acting on the structure, i.e., $n = 1$. Therefore, the specific cost function can be written as:

$$J(\mathbf{u}(\boldsymbol{\kappa})) = \frac{1}{2}\sum_{j=1}^{m} w_j(\mathbf{u}_j^{\text{meas}} - \underline{\mathbf{I}}_j \cdot \mathbf{u}(\boldsymbol{\kappa}))^2 \quad . \tag{2}$$

The FE residual ($\mathbf{R}$), which accounts for nonlinear behaviour and initial stress state ($\boldsymbol{\sigma}_0$), and its change w.r.t. the design variables can be formulated as:

$$\mathbf{R} = \mathbf{f}_{\text{ext}} - \mathbf{f}_{\text{int}}(\mathbf{u}(\boldsymbol{\kappa}), \boldsymbol{\sigma}_0(\boldsymbol{\kappa}), \boldsymbol{\kappa}) = \mathbf{0}, \quad \frac{d\mathbf{R}}{d\boldsymbol{\kappa}} = \frac{\partial \mathbf{R}}{\partial \boldsymbol{\kappa}} + \frac{\partial \mathbf{R}}{\partial \mathbf{u}} \cdot \frac{d\mathbf{u}}{d\boldsymbol{\kappa}} = \mathbf{0}. \tag{3}$$

The Lagrangian formulation from (2) is written as:

$$\mathcal{L} = J + \tilde{\mathbf{u}}^t \cdot \mathbf{R} \quad . \tag{4}$$

Using the variational differentiation of the Lagrangian w.r.t. its unknowns, the forward problem (from $\frac{\partial \mathcal{L}}{\partial \tilde{\mathbf{u}}} = \mathbf{R} = \mathbf{0}$) and the adjoint problem (from $\frac{\partial \mathcal{L}}{\partial \mathbf{u}} = \mathbf{0}$) are obtained. The adjoint problem can be written as:

$$\left[-\frac{\partial \mathbf{R}}{\partial \mathbf{u}}\right]^t \cdot \tilde{\mathbf{u}} = \frac{\partial J}{\partial \mathbf{u}} \implies \underline{\mathbf{K}}_{\text{tangent}}^t \cdot \tilde{\mathbf{u}} = \frac{\partial J}{\partial \mathbf{u}} \quad , \tag{5}$$

where $\underline{\mathbf{K}}_{\text{tangent}}$ is symmetric for most structural systems, allowing its reuse for the adjoint solve. The gradient can be calculated by using $\frac{d\mathbf{R}}{d\boldsymbol{\kappa}} = \mathbf{0}$ and $\frac{d\mathbf{u}}{d\boldsymbol{\kappa}}$ from (3), rearranging the brackets and inserting $\tilde{\mathbf{u}}^t$ from (5):

$$\begin{aligned} \frac{d\mathcal{L}}{d\boldsymbol{\kappa}} = \frac{dJ}{d\boldsymbol{\kappa}} &= \frac{\partial J}{\partial \boldsymbol{\kappa}} + \left(-\frac{\partial J}{\partial \mathbf{u}} \cdot \left[\frac{\partial \mathbf{R}}{\partial \mathbf{u}}\right]^{-1}\right) \cdot \frac{\partial \mathbf{R}}{\partial \boldsymbol{\kappa}} \\ &= \frac{\partial J}{\partial \boldsymbol{\kappa}} + \tilde{\mathbf{u}}^t \cdot \frac{\partial \mathbf{R}}{\partial \boldsymbol{\kappa}} \quad . \end{aligned} \tag{6}$$

The system identification parameter vector $\boldsymbol{\kappa}$ for constitutive and prestress parameters identification for a linear elastic orthotropic 2D model contains the orthotropic Young's moduli, Poisson's ratio, shear modulus, and prestresses in the warp and weft directions ($\boldsymbol{\kappa} = [E_{\text{warp}}, E_{\text{weft}}, \nu, G, P_{\text{warp}}, P_{\text{weft}}]$). It influences the gradient through the residual as $\mathbf{R}(\boldsymbol{u}(\boldsymbol{\kappa}), \boldsymbol{\sigma}_0(\boldsymbol{\kappa}), \boldsymbol{\kappa})$ from (3), where the internal force gets affected by the change of these parameters.

2.2 Optimization

The cost function and the sensitivities calculated using the adjoint methods are used to drive the optimization process as:
(1) Solve the n forward problems corresponding to n load cases to obtain n displacement fields,
(2) solve the n adjoint problems corresponding to n load cases to obtain n sets of adjoint variables,
(3) calculate the n gradient vectors for each of the n load cases,
(4) aggregate & smoothen (if necessary) the n gradient vectors to obtain a single smoothed gradient vector $\frac{dJ^{\text{smooth}}}{d\boldsymbol{\kappa}}$, and
(5) update the parameters based on the step size α as $\rightarrow \boldsymbol{\kappa}_{new} = \boldsymbol{\kappa}_{old} - \alpha \cdot \frac{dJ^{smooth}}{d\boldsymbol{\kappa}}$.

The search direction is scaled by the gradient's L_2 norm (Ref. [7]). Here, Barzilai-Borwein (BB) step method is used to calculate the step size for the iteration i based on the previous parameter update ($\mathbf{d}^{(i-1)} = \boldsymbol{\kappa}^{(i)} - \boldsymbol{\kappa}^{(i-1)}$) and change of gradient ($\mathbf{y}^{(i)} = \nabla J(\boldsymbol{\kappa}^{(i)}) - \nabla J(\boldsymbol{\kappa}^{(i-1)})$) as $\alpha^{(i)} = \frac{\mathbf{d}^{(i-1),t} \cdot \mathbf{d}^{(i-1)}}{\mathbf{d}^{(i-1),t} \cdot \mathbf{y}^{(i)}}$. For high-fidelity parameter identification, where the number of parameters to be identified is much higher, the optimization becomes highly ill-conditioned and may require smoothing and regularization techniques (further explanation in Ref.[4;6;7]).

3 EXAMPLES

Two examples are presented here, a simple Hypar and a Conic example, to demonstrate the approach's applicability for constitutive parameters and prestress parameters identification. The examples are loosely based on the Round Robin exercise[1], which was conducted for the analysis and design of membrane structures. Kratos Multiphysics[8;9], an open-source FE framework, is used for the implementation. For all the cases, a 'target' parameter vector is prescribed, and the displacements are obtained at the sensor locations. This data is recorded as the 'measured data' in the cost function, which the optimization algorithm minimizes by tuning the design parameters $\boldsymbol{\kappa}$ to obtain the 'identified' parameter vector. For all the cases, the steepest descent algorithm with

Table 1: Fixed parameters of the membrane structure used in all examples in this work. These parameters were kept constant and are not part of the system identification variables.

Category	Parameter	Value	Unit
Membrane			
	Thickness	1	mm
Cables			
	Young's modulus	205	GPa
	Cable diameter	12	mm
	Cable Prestress	30	kN
Loads			
	Uniform wind uplift (perpendicular to upper surface of fabric)	1.0	kN/m^2
	Uniform snow load (vertically downwards)	0.6	kN/m^2

Note: The membrane thickness given above is used to convert the membrane stiffness and shear modulus values expressed in kN/m to equivalent values in kN/m^2 and used in this work.

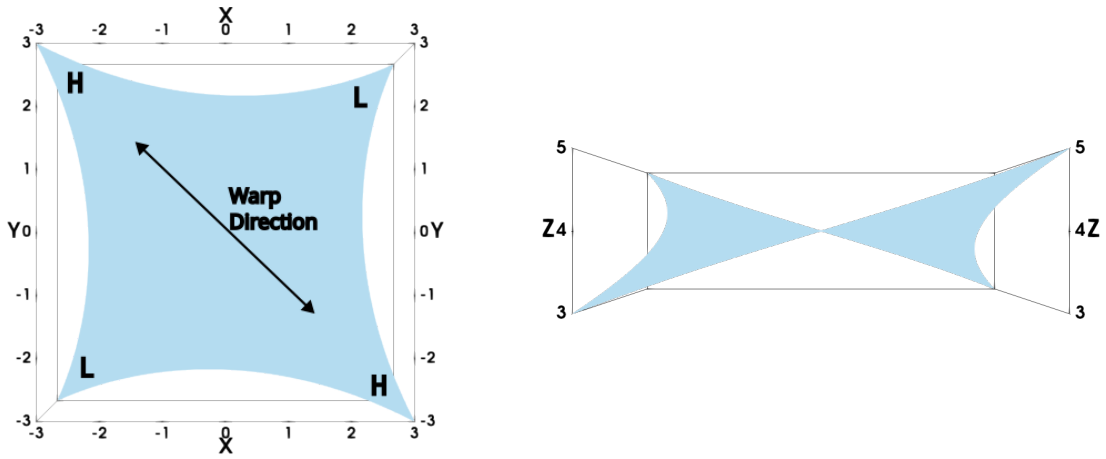

Figure 1: **Hypar Example.** Top (left) and Side (right) View of the Model Setup. "H" Indicates the High-Points and "L" Indicates the Low-Points of the Hypar.

BB max. step of 1.0 is used for the optimization with a stopping criterion of either the cost function $< 1.0E-16$ or maximum iterations of 2000.

Additionally, some parameters, such as the membrane thickness, edge cable diameter and mechanical properties, and external loads, are kept fixed (not part of system identification) and are the same for all the example cases. These parameters are shown in Table 1. It is also noted that, for membrane structures, the stiffness and shear modulus are generally reported in kN/m. In this work, these quantities are converted (using membrane thickness) to equivalent values in kN/m^2 to conform with the FE code input.

3.1 Hypar Example

This example is shown in Figure 1. The 4-point Hypar structure has two low points and two high points. The structure dimensions are 6 m, 6 m, and 2 m in the x, y, and z directions, respectively. The hypar is fixed at the four corners. 3910 triangular membrane elements and 336 cable elements

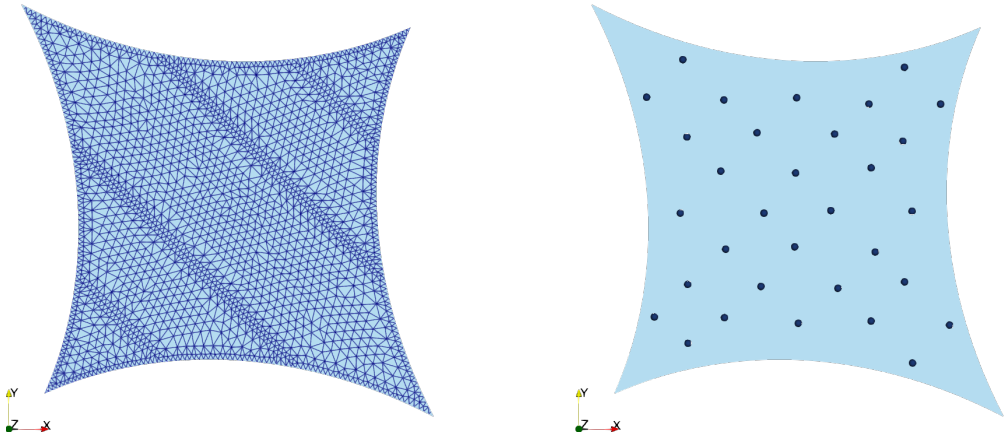

Figure 2: **Hypar Example.** Model Mesh (left) and the 32 Displacement Sensors Locations (right).

are used to discretize the membrane and edge cables of the structure, respectively. Due to the small thickness, the membrane is simulated under a plane stress condition. Figure 2 shows the FE mesh and the 32 displacement sensors distributed over the hypar surface with equal weightings of $w = 100$ in the cost function.

Two different types of material and prestress behaviors are tested for the Hypar: 1) Equal prestresses and equal Young's moduli in warp and weft directions (but independent shear modulus), and 2) Asymmetric prestresses and orthotropic Young's moduli in warp and weft directions.

3.1.1 Hypar with Equal Prestress and Pseudo-Isotropic Material

In this case, the material is referred to as 'pseudo-isotropic' because even though the Young's moduli in the warp and weft directions are equal, the material does not follow the isotropic relation for shear modulus ($G = E/(1+\nu)$), and is specified independently, thus showing pseudo-isotropic behavior. This is common for membranes that have a reduced shear modulus. The prestress in the warp and weft directions is also prescribed to be equal and uniform. Therefore, in this case, there are four independent design parameters ($E_{\text{warp}} = E_{\text{weft}}, \nu, G, P_{\text{warp}} = P_{\text{weft}}$) whose target values are shown in Table 2. The initial values of the parameters at the beginning of the identification are: $E_{\text{warp,0}} = E_{\text{weft,0}} = 5.8E + 06$ N/m², $\nu_0 = 3.8E - 01, G_0 = 2.8E + 07$ N/m², and $P_{\text{warp,0}} = P_{\text{weft,0}} = 2.8E + 06$ N/m. Table 2 shows the results for the parameters identification for this case. It can be observed that all four parameters have identified values very close to the target values. The percentage error is less than 0.2% for all variables.

Table 2: **Hypar Example.** Case 1: Equal Prestress and Equal Young's Moduli. Identified membrane material parameters and prestress under different load conditions.

Independent Design Parameters	Target Value	Unit	Prestress + Wind Load		Prestress + Snow Load	
			Identified Value	Percentage Error	Identified Value	Percentage Error
$E_{\text{warp}} = E_{\text{weft}}$	6.00E+08	N/m²	6.0005E+08	8.79E-03	5.9985E+08	2.57E-02
ν	4.00E-01	–	4.0013E-01	3.18E-02	3.9964E-01	8.94E-02
G	3.00E+07	N/m²	2.9987E+07	4.35E-02	3.0042E+07	1.40E-01
$P_{\text{warp}} = P_{\text{weft}}$	3.00E+06	N/m	2.9997E+06	1.103E-02	3.0006E+06	2.15E-02

3.1.2 Hypar with Asymmetric Prestress and Orthotropic Material

In this case, the Young's moduli in the warp and weft directions are unequal. Here, a 10% orthotropy is considered i.e., $E_{\text{warp}} = 1.1 \cdot E_{\text{weft}}$. The prestress in the warp and weft directions is prescribed to be unequal, but uniform in each direction. Although in reality, the Poisson's ratio may not conform[1] to the reciprocal relation ($\nu_{\text{warp-weft}}/E_{\text{warp}} = \nu_{\text{weft-warp}}/E_{\text{weft}}$), in this study, it is considered that $\nu_{\text{warp-weft}} = \nu_{\text{weft-warp}}$, and henceforth denoted as ν. Therefore, in this case,

Table 3: **Hypar Example.** Case 2: Asymmetric Prestress and Orthotropic Young's Modulus. Identified membrane material parameters and prestresses under different load conditions.

Independent Design Parameters	Target Value	Unit	Prestress + Wind Load		Prestress + Snow Load	
			Identified Value	Percentage Error	Identified Value	Percentage Error
E_{warp}	6.00E+08	N/m²	5.9375E+08	1.04E+00	6.0098E+08	1.64E-01
E_{weft}	5.45E+08	N/m²	5.4350E+08	2.75E-01	5.4592E+08	1.69E-01
ν	4.00E-01	-	3.9001E-01	2.50E+00	4.00003E-01	6.66E-04
G	3.00E+07	N/m²	3.0362E+07	1.21E+00	3.0013E+07	4.41E-02
P_{warp}	3.00E+06	N/m	3.0021E+06	6.96E-02	2.9959E+06	1.37E-01
P_{weft}	2.00E+06	N/m	2.0028E+06	1.40E-01	2.0012E+06	6.21E-02

there are six independent design parameters ($E_{\text{warp}}, E_{\text{weft}}, \nu, G, P_{\text{warp}}, P_{\text{weft}}$) whose target values are shown in Table 3. The initial values of the parameters at the beginning of the identification are: $E_{\text{warp},0} = 5.8E + 06$ N/m², $E_{\text{weft},0} = 5.8E + 06$ N/m², $\nu_0 = 3.8E - 01, G_0 = 2.8E + 07$ N/m², $P_{\text{warp},0} = 2.8E + 06$, and $P_{\text{weft},0} = 1.8E + 06$ N/m. Table 3 shows the results for the parameters identification for this case. In this case also, all six parameters have identified values close to their target values. It can also be observed that identification under snow load has smaller percentage errors than the values obtained under wind load, indicating that the load type and intensity may also play a role in the accuracy of the identification.

3.2 Conic Example

This example is shown in Figure 3. The Conic dimensions are 6 m, 6 m, and 2 m in the x, y, and z directions, respectively, with a circular head ring at the top, having a diameter of 1.6 m. The

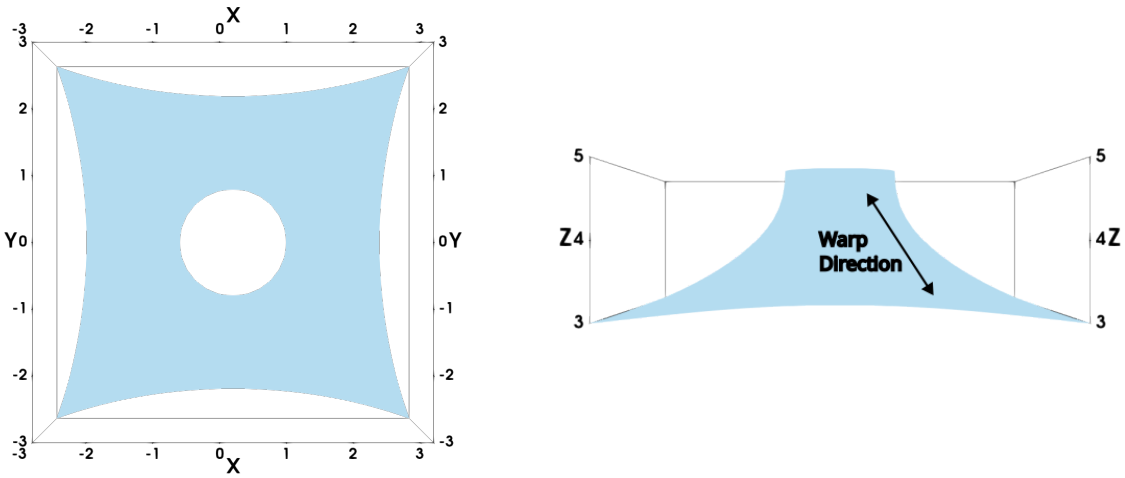

Figure 3: **Conic Example.** Top (left) and Side (right) View of the Model Setup.

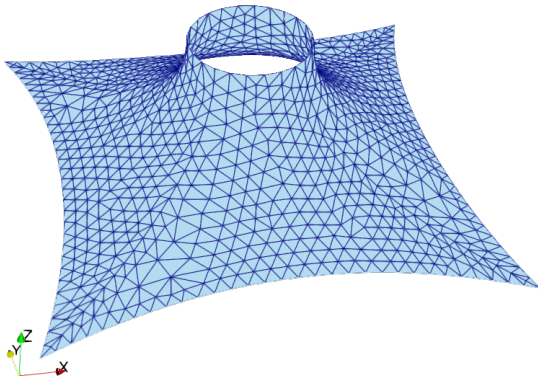

Figure 4: **Conic Example.** Model Mesh

Conic is fixed at the four corners at the base and the circular head ring at the top. 1844 triangular membrane elements and 124 cable elements are used to discretize the membrane and edge cables at the bottom of the structure, respectively, as shown in Figure 4. Due to the small thickness, the membrane is simulated under a plane stress condition. Figure 5 shows the 36 displacement sensors distributed over the conic surface with equal weightings of $w = 100$ in the cost function.

Similar to the Hypar example, two different types of material and prestress behaviors are tested: 1) Equal prestresses and equal Young's moduli in warp and weft directions (but independent shear modulus), and 2) Asymmetric prestresses and orthotropic Young's moduli in warp and weft directions.

3.2.1 Conic with Equal Prestress and Pseudo-Isotropic Material

As explained earlier in Section 3.1.1 about the pseudo-isotropic nature of this case, in this example, the Young's moduli in the warp and weft directions are equal and with an independent

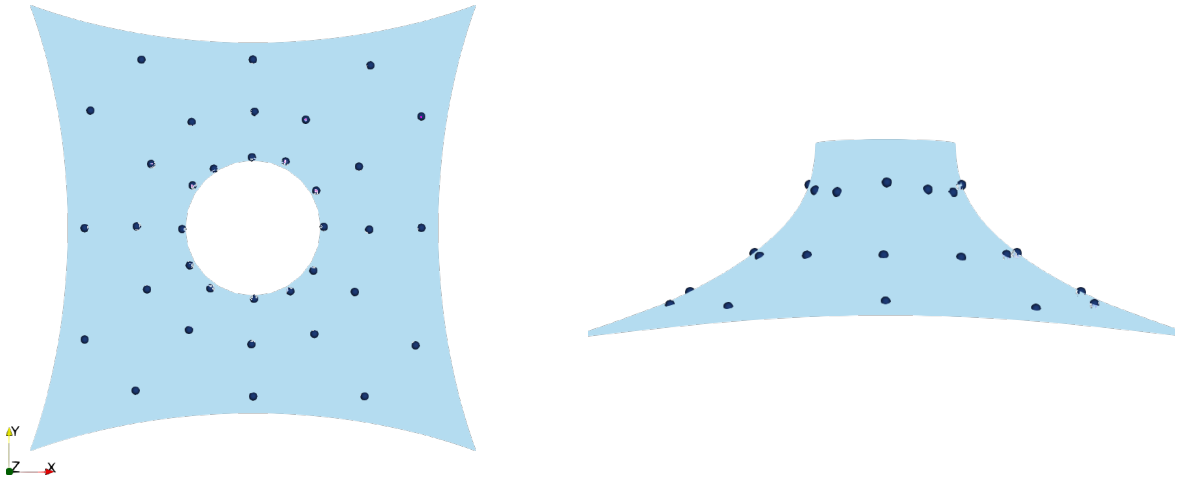

Figure 5: **Conic Example.** Top (left) and Side (right) View of the 36 Displacement Sensor Locations.

Table 4: **Conic Example.** Case 1: Equal Prestress and Equal Young's Moduli. Identified membrane material parameters and prestress under different load conditions.

Independent Design Parameters	Target Value	Unit	Prestress + Wind Load		Prestress + Snow Load	
			Identified Value	Percentage Error	Identified Value	Percentage Error
$E_{\text{warp}} = E_{\text{weft}}$	6.00E+08	N/m²	5.99999999E+08	1.18E-07	6.0000001E+08	1.79E-06
ν	4.00E-01	-	4.00000056E-01	1.41E-05	4.0000032E-01	7.96E-05
G	3.00E+07	N/m²	2.99999973E+07	8.94E-06	3.0000003E+07	8.69E-06
$P_{\text{warp}} = P_{\text{weft}}$	4.00E+06	N/m	4.00000009E+06	2.20E-06	3.9999994E+06	1.42E-05

shear modulus. The prestress in the warp and weft directions is also prescribed to be equal and uniform. This results in four independent design parameters ($E_{\text{warp}} = E_{\text{weft}}, \nu, G, P_{\text{warp}} = P_{\text{weft}}$) whose target values are shown in Table 4. The initial values of the parameters at the beginning of the identification are: $E_{\text{warp,0}} = E_{\text{weft,0}} = 5.8E+06$ N/m², $\nu_0 = 3.8E-01, G_0 = 2.8E+07$ N/m², and $P_{\text{warp,0}} = P_{\text{weft,0}} = 3.8E+06$ N/m. Table 4 shows the results for the parameters identification for this case. It can be observed that all four parameters have identified values that are extremely close to the target values, with percentage errors in the range of 10^{-5} - 10^{-7} for all the variables.

3.2.2 Conic with Asymmetric Prestress and Orthotropic Material

Lastly, in this case, the Young's moduli in the warp and weft directions are unequal, with a 10% orthotropy ($E_{\text{warp}} = 1.1 \cdot E_{\text{weft}}$) considered. The prestress in the warp and weft directions is prescribed to be unequal, but uniform in each direction. The target values for the six independent design parameters ($E_{\text{warp}}, E_{\text{weft}}, \nu, G, P_{\text{warp}}, P_{\text{weft}}$) are shown in Table 5. The initial values of the parameters at the beginning of the identification are: $E_{\text{warp,0}} = 5.8E+06$ N/m², $E_{\text{weft,0}} = 5.8E+06$

Table 5: **Conic Example.** Case 2: Asymmetric Prestress and Orthotropic Young's Modulus. Identified membrane material parameters and prestresses under different load conditions.

Independent Design Parameters	Target Value	Unit	Prestress + Wind Load		Prestress + Snow Load	
			Identified Value	Percentage Error	Identified Value	Percentage Error
E_{warp}	6.00E+08	N/m²	6.0007E+08	1.21E-02	6.0036E+08	5.95E-02
E_{weft}	5.45E+08	N/m²	5.4515E+08	2.78E-02	5.4529E+08	5.24E-02
ν	4.00E-01	-	3.9982E-01	4.47E-02	3.9945E-01	1.38E-01
G	3.00E+07	N/m²	2.9999E+07	2.06E-03	3.0001E+07	2.43E-03
P_{warp}	4.00E+06	N/m	3.99997E+06	7.79E-04	4.0024E+06	6.12E-02
P_{weft}	2.00E+06	N/m	2.00002E+06	1.20E-03	1.9990E+06	5.23E-02

N/m², $\nu_0 = 3.8E-01, G_0 = 2.8E+07$ N/m², $P_{\text{warp},0} = 3.8E+06$, and $P_{\text{weft},0} = 2.2E+06$ N/m. Table 5 shows the results for the parameters identification for this case. In this case also, all six parameters have identified values close to their target values. No significant difference is observed in the results obtained from the different load cases.

4 CONCLUSIONS

This work proposes an adjoint-based, optimization-driven approach for identifying constitutive parameters and prestress in membrane structures for model calibration. The parameter identification problem is set up such that the cost function to be minimized contains the errors between the sensor data and the model response; the gradients are calculated efficiently using the adjoint method where the number of system solves depends on the number of responses rather the number of design variables. In this work, the computational gain of the adjoint calculation may not be huge since the number of design variables is 4 or 6, however, it lays the basis for enormous computing efficiency when extending this methodology for high-fidelity identification problems.

A four-point Hypar and a Conic examples are used to demonstrate the approach's effectiveness. The examples are tested for pseudo-isotropic (equal Young's moduli but independent shear modulus) and orthotropic material behavior with equal and asymmetric prestress, respectively. The prestresses are assumed to be uniform in each direction. For the parameter identification, orthotropic Young's moduli, Poisson's ratio, shear modulus, and the prestresses in the warp and weft directions are considered. In this preliminary study, single values of these parameters for the entire structure are identified, i.e., low-fidelity identification. Both examples are tested with two different external loads (snow and wind uplift). In all cases, the identified values of the design parameters showed close agreement with the target values. In general, the equal prestress with pseudo-isotropic material case produced better results due to fewer design variables (since the Young's moduli and prestress are equal in the warp and weft directions). It is also observed that, in most cases, Poisson's ratio and shear modulus are the most difficult to identify i.e., have the highest errors when compared to other parameters. This is in line with the findings of Ref.[2].

Overall, the methodology works accurately for this low-fidelity identification of material parameters and prestresses in membrane structures. Despite promising results, several challenges remain:

- Can this methodology be applied to non-linear and anisotropic membrane materials?
- In practice, uniform membrane prestress is seldom achieved[1], therefore, can non-uniform prestress be identified?
- What is the optimal type, number, and placement of sensors, and how does their added mass influence the structural response?
- How to improve navigation through the multi-modal terrain to get closer to the global optimum during system identification?

5 ACKNOWLEDGEMENT

This work is funded by SIEMENS AG and the Technical University of Munich, Institute for Advanced Study, Lichtenbergstrasse 2a, D-85748, Garching, Germany. It is also partially supported by ONR under Award NO: N00014-24- 1-2147, NSF grant DMS-2408877, and AFOSR under Award NO: FA9550-25-1-0231 . We would like to acknowledge the funding by the Deutsche Forschungsgemeinschaft under German's Excellence Strategy - EXC 2163/1 - Sustainable and Energy Efficient Aviation - Project-ID 390881007.

REFERENCES

[1] Gosling PD, Bridgens BN, Albrecht A, Alpermann H, Angeleri A, Barnes M, Bartle N, Canobbio R, Dieringer F, Gellin S, Lewis W, Mageau N, Mahadevan R, Marion J-M, Marsden P, Milligan E, Phang YP, Sahlin K, Stimpfle B, Suire O, Uhlemann J (2013). Analysis and design of membrane structures: results of a round robin exercise. Engineering Structures, 48, 313-328.

[2] Battaglia, G., Di Matteo, A., Micale, G., & Pirrotta, A. (2021). Analysis of Rectangular Orthotropic Membranes for Mechanical Properties Identification through Load-Displacement Data. Journal of Engineering Mechanics, 147(6), 04021028.

[3] Liu, C. J., Todd, M. D., Zheng, Z. L., & Wu, Y. Y. (2018). A nondestructive method for the pretension detection in membrane structures based on nonlinear vibration response to impact. Structural Health Monitoring, 17(1), 67-79.

[4] Löhner, R., Airaudo, F., Antil, H., Wüchner, R., Meister, F., & Warnakulasuriya, S. (2024). High-fidelity digital twins: Detecting and localizing weaknesses in structures. International Journal for Numerical Methods in Engineering, 125(21), e7568.

[5] Ansari, T. S. A., Warnakulasuriya, S., Wüchner, R., Bletzinger, K. U., Antonau, I., Löhner, R., Antil, H. & Airaudo, F. (2025). Adjoint-based system identification for model validation and qualification. In Engineering Materials, Structures, Systems and Methods for a More Sustainable Future (pp. 1392-1397). CRC Press.

[6] Ansari, T. S. A., Löhner, R., Wüchner, R., Antil, H., Warnakulasuriya, S., Antonau, I., & Airaudo, F. (2025). Adjoint-based recovery of thermal fields from displacement or strain measurements. Computer Methods in Applied Mechanics and Engineering, 438, 117818.

[7] Antonau, I., Warnakulasuriya, S., Wuechner, R., Airaudo, F., Lohner, R., Antil, H., & Ansari, T. (2025). Comparison of the First Order Algorithms to Solve System Identification Problems of High-Fidelity Digital Twins. In AIAA SCITECH 2025 Forum (p. 0285).

[8] Dadvand, P., Rossi, R., & Oñate, E. (2010). An object-oriented environment for developing finite element codes for multi-disciplinary applications. Archives of computational methods in engineering, 17(3), 253-297.

[9] Vicente Mataix Ferrándiz, Philipp Bucher, Rubén Zorrilla, Suneth Warnakulasuriya, Alejandro Cornejo, Riccardo Rossi, Carlos Roig, jcotela, Josep Maria, tteschemacher, Miguel Masó, Guillermo Casas, Marc Núñez, Pooyan Dadvand, Salva Latorre, Ignasi De Pouplana, Joaquín Irazábal González, AFranci, Ferran Arrufat, … jgonzalezusua. (2025). KratosMultiphysics/Kratos: v10.2.3 (v10.2.3). Zenodo. https://doi.org/10.5281/zenodo.15687676